Large efficiency at telecom wavelength for optical quantum memories

Julián Dajczgewand, Jean-Louis Le Gouët, Anne Louchet-Chauvet, and Thierry Chanelière*

Laboratoire Aimé Cotton, CNRS-UPR 3321, Université Paris-Sud, Bât. 505, 91405 Orsay cedex, France

**Corresponding author: thierry.chaneliere@u-psud.fr*

Received December 3, 2013; revised March 28, 2014; accepted March 28, 2014;
posted April 1, 2014 (Doc. ID 202428); published April 25, 2014

We implement the ROSE protocol in an erbium-doped solid, compatible with the telecom range. The ROSE scheme is an adaptation of the standard two-pulse photon echo to make it suitable for a quantum memory. We observe a retrieval efficiency of 40% for a weak laser pulse in the forward direction by using specific orientations of the light polarizations, magnetic field, and crystal axes. © 2014 Optical Society of America

OCIS codes: (020.1670) Coherent optical effects; (160.5690) Rare-earth-doped materials; (160.2900) Optical storage materials; (210.4680) Optical memories; (270.5565) Quantum communications; (270.5585) Quantum information and processing.

http://dx.doi.org/10.1364/OL.39.002711

The use of erbium-doped materials has revolutionized fiber-optic communications. The erbium-doped fiber amplifier is a key enabling technology already emblematic of our century. Its transposition to the quantum communication world is an active subject of research showing interesting possibilities for long-distance quantum cryptography [1,2].

The direct use of erbium-doped fibers as an optical quantum memory is extremely appealing. Nevertheless, the coherence time necessary to preserve the quantumness falls in the microsecond range even at sub-Kelvin temperature [3]. Instead of amorphous materials [4], crystalline samples, namely Er^{3+}:Y_2SiO_5, have shown remarkably long optical coherence time for solids [5]. These engaging properties are unfortunately counterbalanced by poor optical pumping dynamics. Spectral hole-burning (SHB) required by most of the quantum storage protocols is particularly challenging in erbium-doped solids [6]. This intrinsic limitation is both due to the short lifetime of the population possibly shelved in the Zeeman sublevels (<100 ms [6]) and to the long excited-state population lifetime (~10 ms). The ratio between the two time scales is not sufficient to obtain a good state preparation for optical thick samples. This simple experimental observation drastically bridles the implementation of quantum memories in the telecom band [7]. As an example, using the protocol named CRIB for controlled reversible inhomogeneous broadening derived from the photon-echo technique, Lauritzen obtained an efficiency of 0.25% in Er^{3+}:Y_2SiO_5 [8] but Hedges reached 69% in Pr^{3+}:Y_2SiO_5 [9] essentially explained by different optical pumping dynamics.

We recently proposed a protocol called revival of silenced echo (ROSE). It does not require any state preparation [10]. ROSE is a sequel of the standard two-pulse echo (2PE) adapted for quantum information storage. The 2PE involves a π-pulse, which has two detrimental consequences. On the one hand, it inverts the population and induces spontaneous and stimulated emission that cannot be fundamentally separated from the signal [11]. On the other hand, the restricting phase-matching condition imposes the beam overlap between the signal and the strong rephasing pulse rendering low noise detection difficult in practice. ROSE gets rid of both: (1) two rephasing pulses bring back the population in the ground state. So the protocol is in principle noise free and in practice limited by the experimental quality of the double excitation and (2) the use of two pulses instead of one relaxes the phase-matching condition. The protocol also advantageously replaces the π-pulses by adiabatic passages with chirped pulses. These latter are more robust with respect to the experimental power fluctuations. As compared to π-pulses, they have been demonstrated to be particularly efficient in absorbing media [12].

As a descendant of the 2PE, ROSE is naturally well adapted to storage into the optically excited states whose coherence times are generally shorter than the ground-state sublevels. This apparent limitation should be discussed with precaution in the case of ROSE. Without state preparation, the whole inhomogeneous broadening is available offering a large multiplexing capacity [13]. This latter can drastically reduce the requirements for a long memory lifetime [14]. In other words, for millisecond-storage memory, the short lifetime can be compensated by a large channel number. Such performances are accessible in Er^{3+}:Y_2SiO_5 with a measured 4.4 ms optical coherence time T_2 [5] and a typical inhomogeneous broadening of 500 MHz corresponding to $\sim 10^6$ possible channels.

Even if we avoid the problem of optical pumping for the state preparation by using an appropriate protocol, Er^{3+}:Y_2SiO_5 is still a challenging material to work with. We did not address this issue in our previous proof-of-principle demonstration [10]. First of all, Y_2SiO_5 is a birefingence biaxial crystal. The use of crossed polarized beams to isolate the signal from the rephasing pulses with a noncollinear configuration required by the ROSE may be delicate. Second, the erbium properties are extremely anisotropic in Y_2SiO_5 because of the low substitution site symmetry of Er^{3+} in this compound [5,15,16]. We first present an appropriate beam, polarization, and magnetic field orientation that allows the implementation of ROSE in this material. We obtain a large storage efficiency $\eta \sim 40\%$, close to the expected maximum for the forward configuration, namely 54% [10], for an optical depth of αL

$$\eta = (\alpha L)^2 e^{-\alpha L}. \quad (1)$$

Er^{3+}:Y_2SiO_5 has been first considered by Macfarlane *et al.* [17] and deeply studied regarding its spectroscopic and dynamic properties by Böttger and coworkers [5,15,16,18]. Y_2SiO_5 has three mutually perpendicular optical extinction axes called $\mathbf{D}_1$, $\mathbf{D}_2$, and $\mathbf{b}$. Erbium substitutes two sites with transitions near 1.5 μm from the ground state $^4I_{15/2}$ to the excited state $^4I_{13/2}$. The site used for the experiment is at 1536.48 nm, referenced as site 1 in Böttger's work: it has the longest coherence time. This site presents a population lifetime of around 10 ms at low temperature and an inhomogeneous linewidth of approximately 500 MHz. We use a 3 mm × 4 mm × 5 mm crystal doped with 50 ppm grown by Scientific Materials Corp., and cooled down in a variable temperature liquid helium cryostat to 1.8 K.

We now list the different orientational constraints:

(i) The magnetic field $\vec{B}$ should be placed in the plane $\mathbf{D}_1$–$\mathbf{D}_2$. Otherwise the crystallographic site 1 splits into two magnetically inequivalent subclasses, thus reducing the optical depth [18]. More precisely in the plane $\mathbf{D}_1$–$\mathbf{D}_2$, $\vec{B}$ should ideally make an angle of 135° with respect to $\mathbf{D}_1$. The large g-factors for both sites at this angle strongly reduce the electron-spin fluctuations [5].

(ii) Crossed polarizations between signal and rephasing are helpful to isolate the echo from the strong rephasing pulses.

(iii) The signal and rephasing should not be collinear, neither copropagating nor counterpropagating, to further reduce the contamination of the echo by strong pulses or their specular reflections. A small angle separating quasi-counterpropating beams is desirable [10]. The phase-matching conditions also ensure that the 2PE potentially emitted after the first rephasing pulse is completely silenced but the ROSE echo (after the second rephasing) is emitted in the signal mode (forward).

The configuration we use (see Fig. 1) satisfies the different conditions.

We place the crystal on a rotating sample holder. We choose the rotation axis as $\mathbf{b}$ and the magnetic field in the cryostat is perpendicular to it by construction. We thus satisfy the first condition (i).

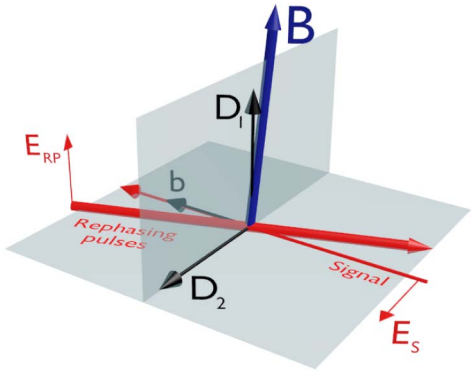

Fig. 1. Beams (signal and rephasing), polarizations (noted E_{RP} and E_S, respectively), and magnetic field $\vec{B}$ orientations. $\mathbf{D}_1$, $\mathbf{D}_2$, and $\mathbf{b}$ are the Y_2SiO_5 optical extinction axes.

We take the signal beam as a reference, it propagates along $\mathbf{b}$. Its polarization is made parallel to $\mathbf{D}_2$ in order to maximize the optical depth for the signal. The absorption is indeed anisotropic. It is weaker along $\mathbf{D}_1$ (by a factor of 2 typically). This is the reason why we polarize the rephasing pulses along $\mathbf{D}_1$. They will be less distorted by the propagation. Cross-polarization is possible in Y_2SiO_5 because the transition dipoles have no preferred orientation neither along $\mathbf{D}_1$ nor along $\mathbf{D}_2$. In other words, the rephasing pulses still act on the dipoles excited by the signal. We fulfill the second condition (ii).

Finally, we slightly deviate from counterpropagating beam configuration for signal and rephasing by setting a few milliradians angle between the two paths. The rephasing beam is then off-axis with respect to $\mathbf{b}$ (signal) but it should be kept in the $\mathbf{b}$ – $\mathbf{D}_1$ or $\mathbf{b}$ – $\mathbf{D}_2$ plane otherwise it will undergo birefringence for geometrical reason. We choose the $\mathbf{b}$ – $\mathbf{D}_2$ plane (see Fig. 1). The last condition (iii) is satisfied.

The magnetic field amplitude should be as large as possible in order to obtain a long coherence time. In our case, the superconducting solenoid inside the cryostat is limited to 3.3 T. With the maximum field we unfortunately cannot use the configuration recommended by Böttger ($\vec{B}$ making a 135° angle with $\mathbf{D}_1$) because our laser has a limited tuning range and cannot go under 1536.12 nm (see below for a complete description). For 3.3 T and $\vec{B}$ making a 135° angle with $\mathbf{D}_1$, the transition is out of reach. Two options are possible to match the laser and the absorption line. Either we keep the 135° angle orientation and reduce the magnetic field or we keep the maximum field of 3.3 T and rotate the crystal to increase the angle to 160° typically. This second option is only possible because the g-factor is strongly anisotropic. It should induce a minor change for the coherence time as described by Böttger. We tested both options and we found that the second presents a larger T_2. It seems better to reduce the g-factor than the magnetic field. This statement deserves further investigation.

The complete experimental setup is described as follows. As a source, we use a commercial erbium-doped fiber laser (Koheras) with a wavelength centered at 1536.5 nm. Its temperature-controlled tuning range is 0.7 nm typically. We split the output of the laser into two beams, one of them was used as the signal (~10 μW) and the other for the rephasing pulses. In order to get strong pulses for the rephasing beam (~10 mW), we inject a erbium-doped fiber amplifier. We adjust the signal and rephasing beam waists to 50 and 110 μm, respectively. We collect the transmitted signal corresponding to the ROSE echo using a monomode fiber and measure it with an avalanche photodiode. Both beams are shaped in time by acousto-optic modulators controlled with a Tektronix AWG520 to provide amplitude and phase control. The time sequence is essentially driven by the maximum available Rabi frequency Ω_0. ROSE involves adiabatic passages as rephasing pulses in the form of complex hyperbolic secant (CHS) [19]. They have a hyperbolic secant shape defined by a time-varying Rabi frequency $\Omega(t) = \Omega_0\,\mathrm{sech}(\beta(t - t_{2,3}))$. The pulses are centered on t_2 and t_3 with a duration $1/\beta$. The frequency is swept around the central frequency ω_0 with an hyperbolic tangent shape $\omega(t) = \omega_0 +$

$\mu\beta\tanh(\beta(t-t_{2,3}))$. The pulse bandwidth is then 2 μβ. The adiabatic condition should be maintained as $\mu\beta^2 \ll \Omega_0^2$ [20].

In practice because the available Rabi frequency is $\Omega_0 \sim 2\pi \times 800$ kHz, we choose $\mu = 1$ and $\beta = 2\pi\times$ 400 kHz. It gives a storage bandwidth of 800 kHz. We set the different delays between the signal at t_1 and the first rephasing pulse $t_{12} = t_2 - t_1 = 4$ μs, the first and the second rephasing pulse $t_{23} = 8$ μs to minimize the overlap between the pulses. The storage time is $2t_{23} = t_3 - t_2 = 16$ μs, much shorter than the expected T_2 (see discussion below). We repeat the experiment every 20 ms, sufficient for the ions to go back to the ground state.

With the specific orientation described previously and the laser at the minimum of its tuning range, 1536.12 nm, we adjust the magnetic field by a few percent around 3.3 T to finely adjust the optical depth to $\alpha L \simeq 2$ where the efficiency should be maximum [Eq. (1)]. We observe the partially absorbed signal at $t_1 = 0$ μs and the ROSE echo at $2t_{23} = 16$ μs (Fig. 2).

We also independently measure the optical depth by using the SHB technique. In Fig. 2, the efficiency is then given by the amplitude ratio between the ROSE echo and transmitted signal multiplied by $\exp(-\alpha L)$: 42% for Fig. 2.

The ROSE efficiency should critically depend on the optical depth αL. To evaluate this dependency we make the crystal absorption vary by probing different frequencies within the inhomogeneous profile. Instead of detuning our Koheras laser by changing its operating temperature, we slightly change the magnetic field by 3% around 3.3 T. It is much faster and more reproducible than tuning the laser. It is sufficient to cover the complete 500 MHz inhomogeneous profile but still small to have no influence on the T_2. For each value of the magnetic field, we independently measure αL by using again the SHB technique. We obtain the efficiency curve in Fig. 3.

The experimental curve can now be compared to the theoretical prediction. To account for the decoherence, we simply modify the efficiency [Eq. (1)] by a factor e^{-4t_{23}/T_2}. We can measure T_2 independently in different ways. First, using the ROSE time sequence, we simply change t_{23} and observe the decay of the echo. It gives $T_2 = 400$ μs. We also use a standard 2PE sequence with strong $\pi/2$ and π-pulses. We then obtain $T_2 = 1.4$ ms. We suspect that this discrepancy is due to instantaneous spectral diffusion, a known interaction effect between

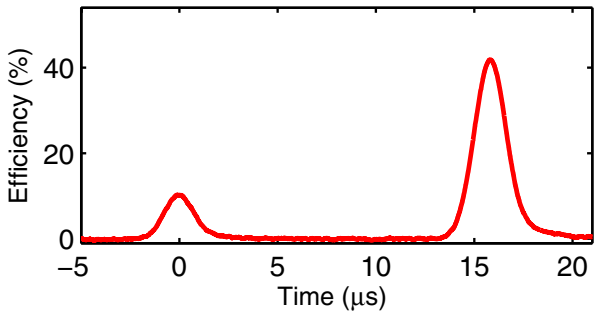

Fig. 2. ROSE echo for $\alpha L = 2.3$. The first pulse is the transmitted signal. The echo is retrieved at $2t_{23} = 16$ μs with an efficiency of 42%.

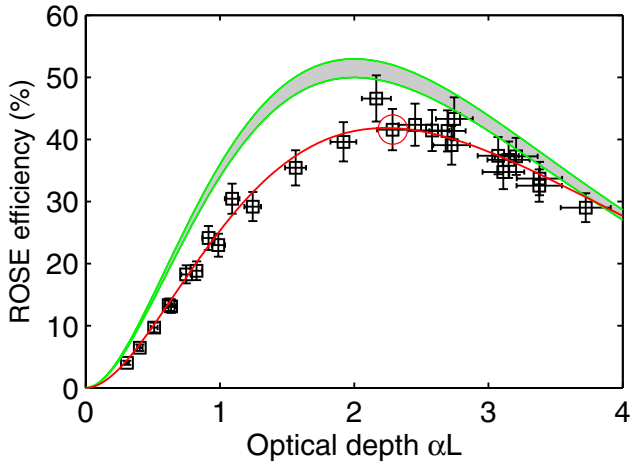

Fig. 3. ROSE efficiency as a function of the optical depth αL. The squares are the experimental data. The error bars essentially come from shot-to-shot fluctuations that we attribute to the laser fluctuations. The data are averaged over a few seconds. The typical deviation of shot-to-shot fluctuations gives the error bar for both the efficiency and αL (from SHB). The solid lines (green and red) represent the fit to theoretical formulas (see text for details). The point corresponding to Fig. 2 is circled.

the erbium ions [18]. This certainly deserves further study but this exceeds the scope of the present paper. Using the two T_2 values, we represent a confidence interval (gray area bounded by the green curves). The qualitative agreement is correct.

We investigate the quantitative discrepancy further by assuming imperfections of the rephasing pulses as compared to Eq. (1), where a complete rephasing is assumed. The task is not easy because the modeling depends on the type of imperfection. We take a simpler approach by analyzing the differential equation leading to Eq. (1), and by introducing phenomenological coefficients. It reads as

$$\frac{d\mathcal{E}(z)}{dz} = -\eta_{\text{pop}}\frac{\alpha}{2}\mathcal{E}(z) + \eta_{\text{phase}}e^{-\frac{2t_{23}}{T_2}}\alpha e^{-\frac{\alpha z}{2}}\mathcal{S}(0), \qquad (2)$$

where $\mathcal{S}$ and $\mathcal{E}$ stand for the signal and the echo amplitude, respectively. We introduce η_{pop} and η_{phase} as phenomenological coefficients justified as follows. The equation is generic and describes the emission of the echo in the forward direction when the medium is in the ground state. It works both for CRIB [21] and ROSE [10]. It can be integrated between 0 and L to obtain the efficiency as $\eta = [\mathcal{E}(L)/\mathcal{S}(0)]^2$. The differential equation can be discussed in physical terms to justify the introduction of η_{pop} and η_{phase}. The first term $(\alpha/2)\mathcal{E}(z)$ describes the attenuation of the echo because the medium is brought back to the ground state. To account for an imperfect return (remaining population), we introduce the factor η_{pop}. The second term in $e^{-(\alpha z/2)}\mathcal{S}(0)$ is a source term. It represents the rephasing of the coherences previously excited by the signal. It decays as $2t_{23}/T_2$ during the storage time $2t_{23}$ because of decoherence. To account for an imperfect rephasing, we introduce η_{phase}. η_{pop} and η_{phase} are clearly phenomenological because we artificially separate the return to the ground state (population)

and the coherence rephasing even though they are due to the same CHS pulses. It has the advantage to provide a simple model to quantify the imperfections of the rephasing stage with *ad hoc* coefficients. After integration, the efficiency can be further simplified by assuming $\alpha L(1-\eta_{\mathrm{pop}}) \ll 1$:

$$\eta \simeq \eta_{\mathrm{phase}}^2 (\alpha L)^2 e^{-\alpha L \frac{1+\eta_{\mathrm{pop}}}{2}} e^{-\frac{4t_{23}}{T_2}}. \quad (3)$$

For $\eta_{\mathrm{pop}} \to 1$ and $\eta_{\mathrm{phase}} \to 1$, one recovers Eq. (1) including the decoherence term. We left these coefficients as free parameters to fit the experimental data. We fix the value of $T_2 = 400$ μs corresponding to the observed ROSE decay. The least square optimization gives the red curve (Fig. 3) with $\eta_{\mathrm{pop}} = 80\%$ and $\eta_{\mathrm{phase}} = 85\%$.

These values are consistent and in good agreement with the inversion quality of the CHS pulse that we measure independently to be consistently in the range 70%–90% [10].

To conclude, we have verified the potential of the ROSE protocol in terms of efficiency. We observe efficient light storage in the telecom range in Er^{3+}:Y_2SiO_5. We have identified an appropriate beam configuration with respect to the crystal axis and magnetic field. On the way toward quantum storage, single photon level measurements should be done to evaluate the noise by spontaneous emission technically limited by the remaining population in the excited state after the rephasing sequence.

We acknowledge financial support from the European program FP7/2007-2013/under REA grant agreement no. 287252 (Marie Curie ITN—CIPRIS) and from the national grant ANR-12-BS08-0015-02 (RAMACO).

References

1. N. Sangouard, C. Simon, H. de Riedmatten, and N. Gisin, Rev. Mod. Phys. **83**, 33 (2011).
2. A. I. Lvovsky, B. C. Sanders, and W. Tittel, Nat. Photonics **3**, 706 (2009).
3. M. U. Staudt, S. R. Hastings-Simon, M. Afzelius, D. Jaccard, W. Tittel, and N. Gisin, Opt. Commun. **266**, 720 (2006).
4. S. R. Hastings-Simon, M. U. Staudt, M. Afzelius, P. Baldi, D. Jaccard, W. Tittel, and N. Gisin, Opt. Commun. **266**, 716 (2006).
5. T. Böttger, C. W. Thiel, R. L. Cone, and Y. Sun, Phys. Rev. B **79**, 115104 (2009).
6. B. Lauritzen, S. R. Hastings-Simon, H. de Riedmatten, M. Afzelius, and N. Gisin, Phys. Rev. A **78**, 043402 (2008).
7. B. Lauritzen, J. c. v. Minář, H. de Riedmatten, M. Afzelius, and N. Gisin, Phys. Rev. A **83**, 012318 (2011).
8. B. Lauritzen, J. c. v. Minář, H. de Riedmatten, M. Afzelius, N. Sangouard, C. Simon, and N. Gisin, Phys. Rev. Lett. **104**, 080502 (2010).
9. M. P. Hedges, J. J. Longdell, Y. Li, and M. J. Sellars, Nature **465**, 1052 (2010).
10. V. Damon, M. Bonarota, A. Louchet-Chauvet, T. Chanelière, and J.-L. Le Gouët, New J. Phys. **13**, 093031 (2011).
11. J. Ruggiero, J.-L. L. Gouët, C. Simon, and T. Chanelière, Phys. Rev. A **79**, 053851 (2009).
12. G. Demeter, Phys. Rev. A **88**, 052316 (2013).
13. J. Nunn, K. Reim, K. C. Lee, V. O. Lorenz, B. J. Sussman, I. A. Walmsley, and D. Jaksch, Phys. Rev. Lett. **101**, 260502 (2008).
14. O. A. Collins, S. D. Jenkins, A. Kuzmich, and T. A. B. Kennedy, Phys. Rev. Lett. **98**, 060502 (2007).
15. T. Böttger, Y. Sun, C. W. Thiel, and R. L. Cone, Phys. Rev. B **74**, 075107 (2006).
16. Y. Sun, T. Böttger, C. W. Thiel, and R. L. Cone, Phys. Rev. B **77**, 085124 (2008).
17. R. M. Macfarlane, T. L. Harris, Y. Sun, R. L. Cone, and R. W. Equall, Opt. Lett. **22**, 871 (1997).
18. T. Böttger, C. W. Thiel, Y. Sun, and R. L. Cone, Phys. Rev. B **73**, 075101 (2006).
19. F. de Seze, F. Dahes, V. Crozatier, I. Lorgeré, F. Bretenaker, and J. L. Le Gouët, Eur. Phys. J. D **33**, 343 (2005).
20. M. F. Pascual-Winter, R.-C. Togning, T. Chanelière, and J.-L. Le Gouët, New J. Phys. **15**, 055024 (2013).
21. N. Sangouard, C. Simon, M. Afzelius, and N. Gisin, Phys. Rev. A **75**, 032327 (2007).